

Postinterventional Assessment after Stent and Flow-Diverter Implantation Using CT: Influence of Spectral Image Reconstructions and Different Device Types

 C. Zaeske,  T. Hickethier,  J. Borggreffe,  L. Goertz,  R. Dettmeyer,  M. Schlamann,  N. Abdullayev, and  C. Kabbasch



ABSTRACT

BACKGROUND AND PURPOSE: CTA provides a noninvasive alternative technique to DSA in the follow-up after endovascular aneurysm treatment to evaluate aneurysm occlusion and exclude intraluminal narrowing after stent or flow-diverter implantation; however, assessability may be impeded by stent material artifacts. The objective of this in vitro study was to compare the visual assessability of different conventional stents and flow diverters as well as different reconstructions of dual-layer CT images.

MATERIALS AND METHODS: Four conventional intracranial stents and 4 flow diverters were implanted in identical aneurysm phantoms. Conventional and monoenergetic images (40, 50, 60, 90, 120, 180 keV) were acquired to evaluate attenuation alteration, visible lumen diameter, and SNR. Image quality was rated subjectively by 2 independent radiologists using a 4-point Likert scale.

RESULTS: Low kiloelectron volt (40–60 keV) monoenergetic reconstructions showed an improved SNR and an improved lumen density ratio compared with high kiloelectron volt reconstructions (90–180 keV) and conventional reconstructions, however without reaching significance compared with the latter. Assessment of the adjacent aneurysm and subjective evaluation was not affected by the imaging technique and stent type. Artifact susceptibility varied with the device used and increased among flow diverters.

CONCLUSIONS: Low kiloelectron volt reconstructions improved the assessment of the stent lumen in comparison with high kiloelectron volt reconstructions. No significant improvement in image quality could be shown compared with conventional images. For some devices, iodine-specific reconstructions led to severe artifacts and are therefore not recommended. There was no relevant improvement in the assessability of the adjacent aneurysm.

ABBREVIATIONS: ID = iodine density; INW = iodine no water

Intracranial stent implantation is a well-established technique for endovascular treatment of intracranial aneurysms, stenoses, and dissections. In the context of stent-assisted coiling, the stent serves as a scaffold that creates a physical barrier between the aneurysm neck and parent vessel to prevent coil migration or protrusion, which can lead to thromboembolic complications.¹ Moreover, the stent can preserve vessel patency and provides more stable aneurysm occlusion, requiring retreatment less frequently than coiling alone.^{1,2} Flow diverters are stents with special architectural properties that were developed to facilitate the

treatment of complex sidewall aneurysms and reduce the rate of associated complications.³ In contrast to the merely supportive use of the stent in the context of stent-assisted coiling, the flow diverter functions as a stand-alone device that leads to consecutive aneurysm closure by flow diversion in the parent vessel and consecutive aneurysm thrombosis across time.³

Despite relevant technical improvements across the years, complications can occur after stent-assisted coiling and flow-diverter implantation, the most important of which are aneurysm remnants, aneurysm recanalization, and in-stent constriction.^{4,5}


DSA represents the criterion standard to evaluate vessel patency and aneurysm occlusion.⁵ However, DSA is an invasive procedure with a low-but-not-negligible complication rate.⁵ A noninvasive and time-saving option for follow-up imaging with lower radiation exposure would therefore be desirable. In contrast, CTA is noninvasive and less time-consuming and has a lower radiation exposure; however, stent-associated artifacts hamper the assessment of the adjacent vessel and aneurysm sac, resulting in a lower diagnostic sensitivity for in-stent stenosis and aneurysm remnants.⁵ These artifacts result from various

Received July 28, 2020; accepted after revision October 12.

From the Institute for Diagnostic and Interventional Radiology (C.Z., T.H., J.B., L.G., M.S., N.A., C.K.) and Center for Neurosurgery (L.G.), Faculty of Medicine, University Hospital Cologne, Cologne, Germany; and Institute of Forensic Medicine (R.D.), Justus-Liebig-University, Giessen, Germany.

N. Abdullayev and C. Kabbasch contributed equally to this work.

Please address correspondence to Charlotte Zaeske, MD, Institute for Diagnostic and Interventional Radiology, University Hospital Cologne, Kerpener Str 62, 50937 Cologne, Germany; e-mail: charlotte.zaeske@uk-koeln.de

 Indicates article with online supplemental data.

<http://dx.doi.org/10.3174/ajnr.A6952>

mechanisms, including beam-hardening, scatter effects, and Poisson noise, with beam-hardening being considered the main factor.⁶ In this context, the extent of the artifacts depends, in particular, on the individual stent type, stent material, and the corresponding x-ray attenuation. By implication, reduction of stent-associated artifacts would presumably increase the diagnostic sensitivity of CTA so that it could be ultimately used as an alternative diagnostic tool to DSA. Previous studies on various medical implants have shown that monoenergetic reconstructions of modern dual-layer CT systems can reduce artifacts significantly.^{6,7}

In contrast to conventional CT, in which the characterization of tissues is based on the respective attenuation of the x-ray spectrum of a certain energy level, dual-energy CT determines the attenuation properties of each tissue at 2 different energy levels, allowing a variety of additional image analyses. One of these additional images is monoenergetic reconstruction, for which many different energy levels can be used. This allows the calculation of the optimal contrasted image data for a particular diagnostic need. The dual-layer CT is a special variant of the dual-energy CT, in which the spectral separation takes place at the level of the detectors so that the dual-energy information is available for each examination, and it shows a high degree of temporal and spatial correlation.⁸ Although a large number of clinical applications have already been described, scientific data on the influence of dual-layer CT on different neuroradiologic stents and its potential to improve image quality of the CTA by artifact reduction are not yet available.

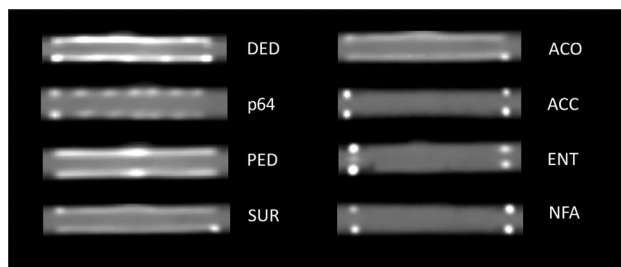


FIG 1. CT of the examined devices. *Left column:* flow diverters. *Right column:* conventional stents. The windowing was adjusted according to the lowest artifact interference of all stents (same settings for all devices).

The objective of this in vitro study was to compare the visual assessability of the aneurysm and stent lumen after implantation of different conventional stents and flow diverters using dual-layer CT image reconstructions.

MATERIALS AND METHODS

Evaluated Devices and Experimental Setup

In preparation for the study, 8 devices (4 flow diverters, 4 conventional stents) were implanted in 8 identical aneurysm phantoms (Fig 1), allowing a comparative analysis of the stent types.

The aneurysm phantoms consisted of a parent vessel with a seated, unilobular, saccular aneurysm with a wall thickness of 0.3 mm. They were manufactured from synthetic resin (Elastic 50A; Formlabs) using a 3D printer, which resulted in density values comparable with those of human vessels in native cranial CT (approximately 30 HU).⁹ The diameter of the parent vessel of the aneurysm phantom was 4 mm with a length of 40 mm, and the aneurysm measured 15 × 10 × 10 mm. The characteristics of the stent types used are shown in Tables 1 and 2 and depicted in Fig 1.

After we manually implanted the devices, the aneurysm phantoms were filled with contrast medium (300 mg iohexol/mL, Accupaque 300; GE Healthcare Buchler GmbH & Co.KG), which was titrated with saline solution to a density value of 280 HU at 120 kV(peak), according to the typically expected vessel density values of an intracranial CTA,¹⁰ and they were sealed at both ends. The models were then positioned in a human skull specimen in a stable position in the area of the sella turcica to simulate artifacts of the skull. This setup was positioned on the CT scanner table in the gantry orthogonal to the z-axis and centered in the middle of the isocenter of the scanner (Online Supplemental Data).

The term “stented” vessel is used to refer to the vessel area in which the device was positioned, regardless of whether a flow diverter or stent was inserted. The term “native” vessel refers to an unstented and artifact-free vessel section.

CT Acquisition Parameters

CT data were acquired on a 64–detector row spectral detector CT scanner (IQon Spectral CT; Philips Healthcare). The same institutional CT protocol used for craniocervical angiography in patients was used for data acquisition (section collimation, 64 ×

Table 1: Details of the flow diverters used in this study

Flow Diverter	Abbreviation	Diameter × Length [mm]	Manufacturer	Main Material	Metal Coverage
Derivo	DED	4 × 24	Acandis	Nitinol, platinum	35%–38%
p64	p64	4 × 40	Phenox	Nitinol	34%
Pipeline Flex with Shield technology	PED	4 × 20	Medtronic	Cobalt chromium, platinum	30%–35%
Surpass Streamline	SUR	4 × 40	Stryker	Cobalt chromium	30%

Table 2: Details of the stents used in this study

Stent	Abbreviation	Diameter × Length [mm]	Manufacturer	Main Material	Metal Coverage
Accero	ACO	4 × 20	Acandis	Nitinol platinum	15%–19%
Acclino Flex Plus	ACC	4 × 35	Acandis	Nitinol	6%–9%
Enterprise 2	ENT	4 × 30	Codman	Nitinol	10%
Neuroform Atlas	NFA	4 × 24	Stryker	Nitinol	6%–9%

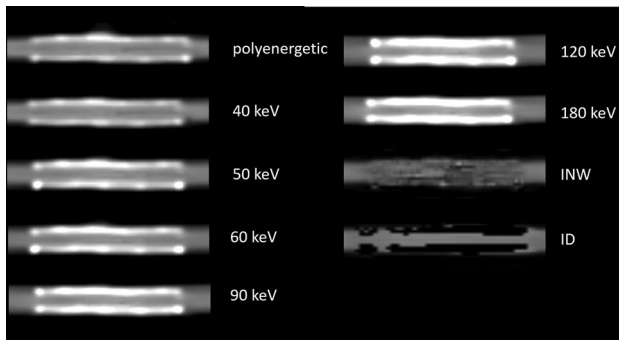


FIG 2. Composition of different reconstructions of the DED. The windowing was adjusted according to the lowest artifact interference and the most comparable vessel appearance (adjusted settings depending on the type of reconstruction; see Materials and Methods, CT Acquisition Parameters).

0.625 mm; rotation time, 0.27 seconds; voltage, 120 kV; tube current–time product, 180 mAs; and resulting CT dose index volume, 16.3 mGy). From the acquired raw data, images were reconstructed using a section thickness of 0.67 mm and an increment of 0.35 mm with a (statistical) hybrid iterative reconstruction algorithm (iDose4; Philips Healthcare) using the iteration level 3, kernel B. Conventional polyenergetic images (120 kVp), virtual monoenergetic images with different energy levels (40, 50, 60, 90, 120, 180 keV), as well as iodine no water (INW) and iodine density (ID) reconstructions were calculated (Fig 2).

Because contrast conditions vary considerably among the different monoenergetic images, individually adjusted window settings for each reconstruction were necessary. Window level and window width were chosen in a joint evaluation session by the 2 readers for an optimized assessment of the stent lumen. With this method, the reviewers jointly determined the most suitable window settings for each type of reconstruction and used them for all similar reconstructions of the different devices. Both subjective and objective evaluations were performed using the specific a priori-determined window settings.

CT Data Analysis

The quantitative data analysis was performed on a separate offline workstation (IntelliSpace Portal; Philips Healthcare).

In the objective analysis, we evaluated the following parameters:

- Lumen width ratio: defined as the visible lumen width of the stented vessel divided by the visible lumen width of the native vessel and measuring the extent of artifact-related restrictions of the assessable vessel lumen
- Lumen density ratio: defined as the density of the stented vessel divided by the density of the native vessel and measuring the extent of artifact-related distortions of the vessel density values. In the case of iodine-specific reconstructions, this parameter is referred to as the lumen iodine content ratio because no density is measured in iodine-specific reconstructions (see below)
- Aneurysm density ratio: defined as the density of the aneurysm divided by the density of the native vessel and measuring

the extent of artifact-related distortions of the aneurysm density values

- Aneurysm neck density ratio: defined as the density of the aneurysm neck adjacent to the stented vessel divided by the density of the native vessel and measuring the extent of artifact-related distortions of the aneurysm neck density values
- SNR: defined as the ratio of the density of the native vessel divided by the image noise (see below for definition of image noise) and measuring the general contrast conditions of the respective reconstruction.

The diameters of the native vessel and the stented vessel were determined for each reconstruction with the previously defined window settings by 2 independent readers and then averaged. The measurements were performed in standardized positions in longitudinal reformations along the centerline of the vessel.

Density measurements with the largest possible ROI (which, however, did not include artifacts or other interfering factors) were performed for all reconstructions and devices at predefined positions as follows: 1) inside the lumen of the aneurysm, 2) in the region of the aneurysm neck (immediately adjacent to the device), 3) within the native vessel lumen, and 4) within the stented vessel lumen (Online Supplemental Data). The corresponding ratios were used to achieve results as comparable as possible with the native vessel as a reference.

With regard to the density ratios, a separate evaluation of the iodine-specific reconstructions was performed because these reconstructions do not measure the density in Hounsfield units, but the iodine content. In INW reconstructions on the one hand, all waterlike substances are suppressed and the measured values are expressed as iodine concentration in milligrams/milliliter. In iodine density reconstructions on the other hand, all pixels that do not contain iodine are suppressed and the iodine concentration is also given in milligrams/milliliter.¹¹

To define image noise, we performed standardized density measurements in an area without any content adjacent to the stent. The obtained SD in this ROI was then defined as image noise.

To allow a first comparison with clinical results, we compared image data from clinical examinations of 2 patients, one with an implanted flow diverter (Derivo embolization device [DED]; Acandis) and one with an implanted conventional stent (Neurform Atlas Stent System [NFA]; Stryker), with the in vitro results of our study with respect to the lumen density ratio and SNR (in both cases the adjacent aneurysm was additionally treated so that it could not be included in the evaluation).

Subjective Analysis

The subjective assessability of the vessel lumen and the aneurysm neck was performed independently by 2 blinded readers. A 4-point Likert scale was used to assess the aneurysm neck: 1) aneurysm neck not definable due to artifacts, no assessment possible; 2) aneurysm neck, in principle, definable, but density appears distorted, limited assessment possible; 3) aneurysm neck definable, residual artifacts, contrast medium intake assessable; 4) aneurysm neck definable, no artifacts, unrestricted assessment. We also assessed the vessel lumen: 1) vessel lumen not definable due to

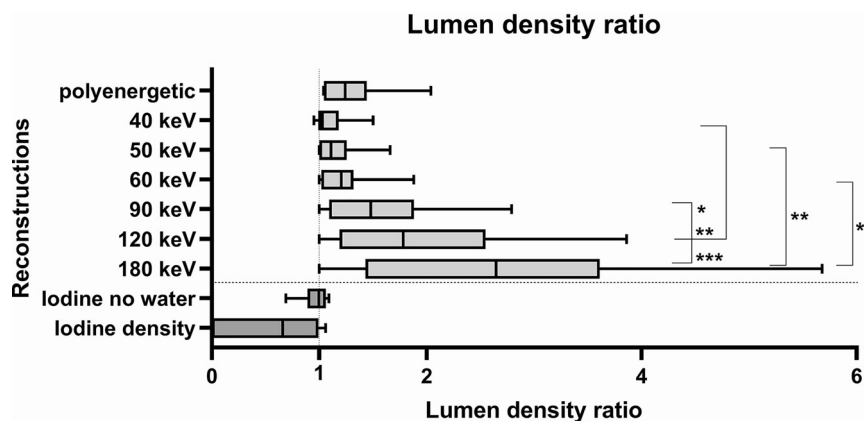


FIG 3. Graphic illustration of the different lumen density ratios/lumen iodine content ratios. Asterisks mark statistical significance (* $P < .05$, ** $P < .01$, *** $P < .001$).

artifacts; 2) vessel lumen, in principle, definable, but density appears to be clearly falsified/not assessable; 3) vessel lumen definable, contrast assessable, residual artifacts; and 4) vessel lumen definable, contrast assessable, no artifacts.

Statistical Analysis

Statistical analysis was performed using GraphPad Prism, Version 8.0.0 for Windows (GraphPad Software). A 2-tailed P value $< .05$ was considered statistically significant. Parametric results are presented as mean [SD].

Normal distribution was tested using the Shapiro-Wilk test. Variances between the devices concerning the continuous data were compared using an ANOVA for matched parametric data with the Greenhouse-Geisser correction to compensate the variability of differences and then using post hoc testing for multiple comparisons by means of the Tukey test. For matched, nonparametric data, we used the Friedman test, with subsequent post hoc testing for multiple comparisons by means of the Dunn test. In the comparison of the iodine-specific reconstructions, we used the Wilcoxon matched-pairs signed rank test.

With regard to the subjective reading, the corresponding weighted Cohen κ was calculated to assess the interobserver agreement. The Cohen κ was rated on the following scale: $\kappa < 0$, no agreement; $\kappa = 0.0$ – 0.2 , slight agreement; $\kappa = 0.21$ – 0.40 , fair agreement; $\kappa = 0.41$ – 0.60 , moderate agreement; $\kappa = 0.61$ – 0.80 , substantial agreement; $\kappa = 0.81$ – 1.00 , almost perfect agreement.¹²

RESULTS

Reconstructions: Objective Reading

Lumen Width Ratio. Reconstructions with 40 and 50 keV had the highest lumen width ratio, with an assessable proportion of about 70% (mean lumen width ratio: 40 keV, 0.73 [SD, 0.21] keV; 50 keV, 0.73 [SD, 0.18] keV); however, the significance was not reached in the comparison with other monoenergetic reconstructions and the conventional polyenergetic images. Significant differences were found between the 40–60 keV reconstructions and the INW and ID reconstructions (40 keV versus INW, $P = .001$; 50 keV versus INW, $P = .006$; 60 keV versus INW, $P = .003$; 40 keV versus ID, $P = .01$; 50 keV versus ID, $P = .04$; 60 keV

versus ID, $P = .02$). For a more detailed description of the results, see the Online Supplemental Data.

Lumen Density Ratio. Low kiloelectron volt monoenergetic reconstructions (40–60 keV) had a lumen density ratio of almost 1.0, which corresponds to an almost undistorted representation of the vessel lumen. Increasing kiloelectron volt values correlated with a higher lumen density ratio, which indicates an increasing distortion of the density of the vessel lumen (Fig 3 and Online Supplemental Data). There were no statistically significant differences in comparison with the

conventional polyenergetic images.

Significant differences were found with regard to the monoenergetic reconstructions when comparing the 40-keV reconstructions with the 90-keV ($P = .03$), 120-keV ($P = .001$), and 180-keV reconstructions ($P < .001$); the 50-keV reconstructions with the 180-keV reconstructions ($P = .006$); and the 60-keV reconstructions with the 180-keV reconstructions ($P = .02$). The conventional, polyenergetic images showed results comparable with the monoenergetic reconstructions in a range between 60 and 90 keV.

Aneurysm and Aneurysm Neck Density Ratio. There were no significant differences regarding the aneurysm and aneurysm neck density ratios. Monoenergetic and polyenergetic reconstructions both resulted in values around 1.0 (exemplarily for 40 keV; mean aneurysm density ratio, 1.07 [SD, 0.09]; mean aneurysm neck density ratio, 1.09 [SD, 0.09]). For a more detailed description of the results, see the Online Supplemental Data.

SNR. Low-energy monoenergetic reconstructions were associated with higher signal-to-noise ratios with a continuous decrease of the values at higher kiloelectron volt levels and the lowest value at 180 keV. The SNRs of the polyenergetic conventional images were within the range of the 50- and 60-keV monoenergetic reconstructions. Because the image noise in the INW and ID reconstructions each resulted in values of zero, no reasonable SNR could be calculated here. Results are graphically illustrated in Fig 4. All of the results can be found in the Online Supplemental Data.

The differences reached a significance level in comparison with the following reconstructions: 40 keV versus 90 keV ($P = .004$), 40 keV versus 120 keV ($P < .001$), 40 keV versus 180 keV ($P < .001$), 50 keV versus 120 keV ($P = .005$), and 50 keV versus 180 keV ($P = .003$).

Iodine-Specific Reconstructions. With regard to the lumen iodine content ratio, the INW reconstructions showed a mean value of 0.96 [SD, 0.13]; and the ID reconstructions, a mean value of 0.54 [SD, 0.50] without reaching a statistically significant level.

The values of the aneurysm iodine content ratio and the aneurysm neck iodine content ratio showed similar mean values of

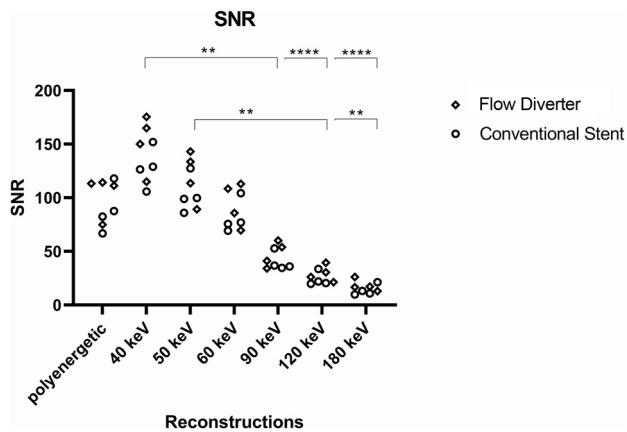


FIG 4. Graphic illustration of the SNR. Asterisks mark statistical significance (* $P < .05$, ** $P < .01$, *** $P < .001$, **** $P < .0001$).

INW and ID reconstructions, respectively (aneurysm iodine content ratio: INW, 1.07 [SD, 0.07]; ID, 1.08 [SD, 0.09]; aneurysm neck iodine content ratio: INW, 1.08 [SD, 0.07]; ID, 1.09 [SD, 0.09]), without significant differences between the reconstructions, either.

Reconstructions: Subjective Reading

The interobserver agreement yielded a weighted Cohen κ of 0.97 for the assessment of the stented vessel and a weighted Cohen κ of 0.97 for the assessment of the aneurysm neck.

Subjective assessability of the vessel lumen and the aneurysm neck was best at 40 keV (vessel lumen, 3.5 [SD, 0.53]; aneurysm neck, 3.69 [SD, 0.46]), and decreased with increasing kiloelectron volt (180 keV: vessel lumen, 3.13 [SD, 0.99]; aneurysm neck, 3.00 [SD, 0.93]). The worst results were obtained for the iodine-specific reconstructions (INW: vessel lumen, 2.38 [SD, 1.51]; aneurysm neck, 2.5 [SD, 1.41]; ID: vessel lumen, 2.50 [SD, 1.41]; aneurysm neck, 2.6 [SD, 1.41]). For a more detailed description of the results, see the Online Supplemental Data.

However, no statistical significance was reached when comparing the subjective assessability of the vessel lumen in the different image reconstructions. With regard to the assessability of the aneurysm neck, a significance level was achieved with the initial Friedman test ($P < .001$) but could then no longer be demonstrated for a specific comparison in the post hoc multiple comparisons.

Devices: Objective Reading

Lumen Width Ratio. A comparison of the different devices in the 40-keV reconstructions, for which vessels and aneurysms showed the best assessability in the previously performed analysis of different reconstructions, revealed that the different devices lead to artifacts of a varying extent. The lowest artifacts with a subsequently high lumen width ratio were found for the Acclino Flex Plus stent (ACC; Acandis), Enterprise stent (ENT; Codman), and NFA (ACC, 0.98; ENT, 0.95; NFA, 0.97). In contrast, the highest amount of artifacts with a consecutively low lumen-width ratio found for the devices DED and Pipeline Embolization Device (PED; Medtronic) were DED at 0.50 and PED at 0.50. The other devices ranged between the above-

mentioned results (Accero stent [ACO], Acandis), 0.68; p64, Phenox, 0.60; and Surpass Streamline flow diverter [SUR], Stryker, 0.62).

Lumen Density Ratio. When comparing the devices at 40 keV, most lumen density ratios were close to 1.0 without relevant differences and only minor deviations for the PED (1.20) and SUR (1.50) devices.

However, the lumen density ratios for the other kiloelectron volt levels showed significant deviations, with a strong increase in kiloelectron volt values, especially for the SUR device (40 keV: 2.04/180 keV: 5.68) and a moderate increase for the ACO (40 keV: 0.95/180 keV: 3.61), DED (40 keV: 1.36/180 keV: 3.61), p64 (40 keV: 1.26/180 keV: 2.30), and PED (40 keV: 1.47/180 keV: 2.99). For the other devices, there was no or only a very small increase (ACC, 40 keV: 0.99/180 keV: 1.49; ENT, 40 keV: 1.00/180 keV: 1.00; NFA, 40 keV: 0.99/180 keV: 1.41). A graphic illustration of the different devices regarding the lumen density ratio in the 40-keV reconstruction can be found in the Online Supplemental Data.

Aneurysm and Aneurysm Neck Density Ratios. Aneurysm and aneurysm neck density ratios were comparable among the reconstructions and individual stent types with values around 1.0, respectively.

Iodine-Specific Reconstructions. With regard to the lumen iodine content ratio, there were strong fluctuations depending on the device. For the INW reconstructions, these were slightly less pronounced, with fluctuations between 0.69 (ACO) and 1.09 (SUR). For the ID reconstructions, these were more evident, with fluctuations between 0.00 (ACO, DED, SUR) and 1.06 (p64). The devices previously described as less susceptible to artifacts were again showing values close to 1.0 in both iodine-specific reconstructions (INW: ACC, 0.9; ENT, 1.00; NFA, 0.98; ID: ACC, 0.97; ENT, 1.00; NFA, 0.97). Regarding aneurysm and aneurysm neck iodine content, INW as well as ID reconstructions showed values around 1.0 for each of the devices without considerable deviation.

Devices: Subjective Reading

The assessability of the vessel lumen in the 40-keV reconstruction was rated as good or very good (4 points: ACC, ACO, ENT, NFA, p64; 3 points: DED, PED, SUR). Corresponding to the results of the objective evaluation, the INW and ID reconstructions in combination with certain devices showed significant limitations in the subjective image quality (ACO, PED, SUR [INW only]), while with other devices (ACC, ENT, NFA), the lumen and aneurysm could be assessed well. The comparison of the different devices with regard to the assessability of the aneurysm neck has led to comparable results and was, therefore, not analyzed separately.

Clinical Findings. A preliminary analysis of clinical data from routine imaging for a flow diverter (DED) and a conventional stent (NFA) showed a course of the lumen density ratio for the flow diverter comparable with that of the in vitro data, with the lowest lumen density ratio at 40 keV and an increase with increasing kiloelectron volt values (Online Supplemental Data).

When we compared the flow diverter and conventional stent, the values obtained for the conventional stent showed significantly less variation among the different reconstructions, which corresponds to the *in vitro* results of the comparison among the different devices. Regarding a preliminary analysis of the SNR, a comparable course of the clinical and *in vitro* data was also observed (Online Supplemental Data) with the best SNR at 40 keV and a decrease of SNR with increasing kiloelectron volt values.

DISCUSSION

The results of this study provide, so far, unavailable information of dual-layer CT imaging of vessels after implantation of intracranial stents and flow diverters. On the one hand, novel data on the benefit of spectral reconstructions of a dual-layer CT could be obtained, and on the other hand, new insights into the influence of different implanted devices on the assessment of the parent vessels and adjacent aneurysms were achieved.

Reconstructions

Our results indicated that monoenergetic reconstructions (without iodine-specific reconstructions) provide better image quality and consequently superior assessment of the stent lumen in the low kiloelectron volt range. This finding was demonstrated by a significantly higher lumen density ratio of low kiloelectron volt reconstructions (40–60 keV) compared with high kiloelectron volt reconstructions (90–180 keV). Likewise, the low kiloelectron volt reconstructions (40–50 keV) had a significantly better SNR compared with the higher kiloelectron volt reconstructions (90–180 keV). An analysis of the lumen width ratio and the subjective assessment of the vessel lumen did not reach the defined significance level; however, it showed a similar trend. In the comparison of monoenergetic and conventional polyenergetic images, significance could not be reached. However, there were pronounced differences among the different devices and their potential for artifact reduction, so further subgroup analyses with larger case numbers and a classification depending on the artifact susceptibility should verify the potential for artifact reduction for particularly artifact-susceptible devices. This point is discussed in more detail in the paragraph “Devices.”

A preliminary analysis of clinical data supports the results regarding the comparison of different reconstructions in terms of lumen density ratio and SNR. Again, the analyzed flow diverters showed the best lumen density ratio and SNR at 40 keV, with a consecutive increase of the lumen density ratio and a decrease of the SNR with rising kiloelectron volt values. It could also be shown that regarding the lumen density ratio, different devices have a different potential for improvement of image quality, shown by considerably less variation in the comparison with different monoenergetic reconstructions in the case of the conventional stent. This is also compatible with the *in vitro* findings, which are discussed in more detail in the section “Devices.”

The findings of a better image quality at lower kiloelectron volt reconstructions seem to contradict the results of a previous study,¹¹ which described better artifact reduction and less image noise at higher kiloelectron volt reconstructions; however, the clinical context must be considered here. Because higher

kiloelectron volt reconstructions are associated with not only fewer artifacts but a higher distance to the iodine k-edge at 33 keV, this finding leads to a decreased SNR as well as a decreased contrast of the vessel lumen, resulting in a reduced assessability of possible in-stent stenosis in comparison with low kiloelectron volt reconstructions. In accordance with these findings, Hickethier et al⁶ already described a reduced contrast-to-noise ratio between nonstenosed and stenosed stent sections and an associated reduced assessability with increasing kiloelectron volt numbers.

Regarding the evaluation of the adjacent aneurysm, both the objective and the subjective reading showed no significant differences between the different reconstructions, so an additional benefit in the clinical evaluation of the aneurysm perfusions or reperfusion seems unlikely.

The iodine-specific reconstructions of some devices allowed an assessment of similar quality as the best monoenergetic and conventional reconstructions and could thus increase the diagnostic certainty as supplementary image information.¹³ With other devices, however, they proved to be more susceptible to artifacts than the monoenergetic images, so they cannot be generally recommended. If more artifacts occurred, this increase led to significantly worse lumen width ratios and distortions of the lumen-iodine content ratio compared with the low kiloelectron volt reconstructions. This scenario could indicate that the corresponding algorithm cannot reliably distinguish iodine and other molecules of higher density in small structures.¹⁴ Overall, the ID reconstruction, in particular, proved to be less reliable than the INW reconstruction, explaining why the latter should be preferred for this purpose.

Devices

On the basis of the results of the different devices that were evaluated here, they can be divided into 3 categories: devices that hardly cause artifacts (ACC, ENT, NFA), devices that lead to moderate artifacts (ACO, p64, SUR), and devices with strongly associated artifacts (DED, PED). Among other things, this finding can be explained by the fact, that most of the artifact prone devices are flow diverters (with the exception of ACO). For the purpose of flow diversion, these must have special architectural properties and be more tightly woven than conventional stents, probably having the disadvantage of inducing stronger artifacts.

The specific architectural properties of flow diverters are defined by the porosity (ratio of open, metal-free area to total stent area) and metal coverage (ratio of metal covered area to total stent area).¹⁵ In accordance with our results, the less artifact-prone devices are laser-cut stents with low metal coverage (ACC, 6%–9%; ENT, 10%; NFA, 6%–9%),¹⁶ while the more artifact-prone devices showed a higher metal coverage, with slightly increased values for the remaining conventional stent (ACO, 15%–19%) and considerably increased values of approximately 30% in the case of the examined flow diverters (DED, 35%–38%; p64, 34%; PED, 30%–35%; SUR, 30%).^{15,17–19}

The material could further contribute to artifact generation. The less artifact-susceptible devices (ACC, NFA, ENT) and the p64, ACO, and DED devices mainly consist of nitinol, which is known to be associated with low radiopacity.²⁰ In contrast, SUR

and PED contain mainly cobalt chromium with a higher radiopacity. In the case of the more artifact-prone devices (DED, PED) as well as the ACO with medium artifact susceptibility, however, an additional use of platinum is said to enhance the fluoroscopic visibility. This characteristic could further contribute to an increased susceptibility to artifacts.

As already suggested by the comparison of the reconstructions, the monoenergetic 40-keV reconstruction proved to be the most suitable for all evaluated devices. For the higher energy reconstructions, the decrease in image quality varied, depending on the individual device. This decrease was particularly pronounced for the SUR device. However, this could also indicate that there is a special potential for artifact reduction or improvement of image quality in this device through the use of particularly suitable reconstructions.

As with the poly- and monoenergetic images, the iodine-specific reconstructions produced artifacts of varying intensity depending on the respective device. Good results were obtained with the devices ACC, NFA, ENT, and p64, while the PED has already shown considerable limitations; for the other devices (ACO, DED, SUR), the iodine content ratio could not be determined at all. This result is also consistent with the artifact susceptibility of the different devices, depending on the respective monoenergetic energy level described above.

Overall, there were more pronounced differences when comparing the devices than when comparing different reconstructions. However, 50% of the devices investigated were conventional stents, which had a low susceptibility to artifacts and a correspondingly low potential for artifact reduction, which may have led to a reduced overall effect of monoenergetic reconstructions on the improvement of image quality and artifact reduction. Further subgroup analyses with larger numbers of cases should, therefore, be conducted in the future.

Limitations

The limitations of the study include the in vitro setting, so potential influences of the surrounding brain parenchyma on the imaging of the aneurysm and the device cannot be addressed. Because there are no recommendations for the windowing of monoenergetic reconstructions in cranial CTAs, these were determined for each reconstruction in a standardized process. In doing so, an attempt was made to do this determination in as standardized and objective a manner as possible, but a certain influence on the results of the lumen width ratio and the subjective results cannot be excluded with certainty. However, this influence is definitely smaller than if unadjusted window settings had been used.

Although preliminary clinical data are included in the study, a larger and more detailed clinical analysis should follow to evaluate the clinical translation. In addition, our model included an untreated aneurysm, so possible differences in the sensitivity of detecting an aneurysm remnant or reperfusion, eg, after aneurysm coiling, cannot be evaluated. Also, with regard to the detection of possible in-stent stenoses, only indirect conclusions can be drawn because a comparison with stenosed vascular phantoms has not been performed. Although our study

already shows promising results, a clinical trial to validate our results is warranted.

CONCLUSIONS

This study provides the first structured data on postinterventional noninvasive imaging of neurointerventional stent devices by CTA using spectral image results of a dual-layer CT. Low-energy monoenergetic reconstructions offer better image quality in comparison with high-energy monoenergetic reconstructions. However, in comparison with conventional images, no significant improvements in image quality could be shown for monoenergetic reconstructions, at least if the individual artifact susceptibility of the devices is not factored in. In this respect, the comparison of the different devices identified ones with low (ACC, ENT, NFA), medium (ACO, p64, SUR), and high (DED, PED) artifact susceptibility. The flow diverters generally proved to be more susceptible to artifacts than conventional stents. The first in vivo data from clinical examination, which were assessed analogous to the study evaluations, seem to support our achieved in vitro results.

Disclosures: Christoph Kabbasch—RELATED: proctor for Acandis and MicroVention. Jan Borggreffe—RELATED: Consulting Fee or Honorarium: honorarium as speaker for scientific lectures from Philips Healthcare.

REFERENCES

1. Mine B, Bonnet T, Vazquez-Suarez JC, et al. **Comparison of stents used for endovascular treatment of intracranial aneurysms.** *Expert Rev Med Devices* 2018;15:793–805 [CrossRef Medline](#)
2. Zhang X, Zuo Q, Tang H, et al. **Stent assisted coiling versus non-stent assisted coiling for the management of ruptured intracranial aneurysms: a meta-analysis and systematic review.** *J Neurointerv Surg* 2019;11:489–96 [CrossRef Medline](#)
3. Briganti F, Leone G, Marseglia M, et al. **Endovascular treatment of cerebral aneurysms using flow-diverter devices: a systematic review.** *Neuroradiol J* 2015;28:365–75 [CrossRef Medline](#)
4. Feng X, Qian Z, Liu P, et al. **Comparison of recanalization and in-stent stenosis between the low-profile visualized intraluminal support stent and Enterprise stent-assisted coiling for 254 intracranial aneurysms.** *World Neurosurg* 2018;109:e99–104 [CrossRef Medline](#)
5. Duarte Conde MP, de Korte AM, Meijer FJ, et al. **Subtraction CTA: an alternative imaging option for the follow-up of flow-diverter-treated aneurysms?** *AJNR Am J Neuroradiol* 2018;39:2051–56 [CrossRef Medline](#)
6. Hicethier T, Wenning J, Bratke G, et al. **Evaluation of soft-plaque stenoses in coronary artery stents using conventional and monoenergetic images: first in-vitro experience and comparison of two different dual-energy techniques.** *Quant Imaging Med Surg* 2020;10:612–23 [CrossRef Medline](#)
7. Hicethier T, Wenning J, Doerner J, et al. **Fourth update on CTA of coronary stents: in vitro evaluation of 24 novel stent types.** *Acta Radiol* 2018;59:1060–65 [CrossRef Medline](#)
8. Rassouli N, Etesami M, Dhanantwari A, et al. **Detector-based spectral CT with a novel dual-layer technology: principles and applications.** *Insights Imaging* 2017;8:589–98 [CrossRef Medline](#)
9. Kamalian S, Lev MH, Gupta R. **Computed tomography imaging and angiography-principles.** *Handb Clin Neurol* 2016;135:3–20 [CrossRef Medline](#)
10. Thust SC, Chong WK, Gunny R, et al. **Paediatric cerebrovascular CTA-towards better image quality.** *Quant Imaging Med Surg* 2014;4:469–44 [CrossRef Medline](#)
11. Romman Z, Yagil Y, Finzi D, et al. **Philips Healthcare: Using spectral results in CT imaging—Philips Iqon Spectral CT.** <https://www.>

philips.co.uk/c-dam/b2bhc/gb/resource-catalog/landing/brightontender/ct-iqon-white-paper-spectral-results-in-ct-imaging-hr.pdf. Accessed March 6, 2020

12. Landis JR, Koch GG. **The measurement of observer agreement for categorical data.** *Biometrics* 1977;33:159 [CrossRef](#) [Medline](#)
13. Weng CL, Tseng YC, Chen DY, et al. **Spectral imaging for intracranial stents and stent lumen.** *PLoS One* 2016;11:e0145999 [CrossRef](#) [Medline](#)
14. Knöß N, Hoffmann B, Krauss B, et al. **Dual energy computed tomography of lung nodules: differentiation of iodine and calcium in artificial pulmonary nodules in vitro.** *Eur J Radiol* 2011;80:e516–19 [CrossRef](#) [Medline](#)
15. Maragkos GA, Dmytriw AA, Salem MM, et al. **Overview of different flow diverters and flow dynamics.** *Neurosurgery* 2020;86:S21–34 [CrossRef](#) [Medline](#)
16. Spiotta AM, Turner RD, Chaudry MI, eds. *Management of Cerebrovascular Disorders.* Springer-Verlag; 2019
17. Sirakov S, Sirakov A, Bhogal P, et al. **The p64 flow diverter—mid-term and long-term results from a single center.** *Clin Neuroradiol* 2020;30:471–80 [CrossRef](#) [Medline](#)
18. De Vries J, Boogaarts J, Van Norden A, et al. **New generation of flow diverter (Surpass) for unruptured intracranial aneurysms: a prospective single-center study in 37 patients.** *Stroke* 2013;44:1567–77 [CrossRef](#) [Medline](#)
19. Beuing O, Lenz A, Donitza A, et al. **Stent-assisted coiling of broad-necked intracranial aneurysms with a new braided microstent (ACCERO): procedural results and long-term follow-up.** *Sci Rep* 2020;10:412 [CrossRef](#) [Medline](#)
20. Boese A, Rose G, Friebe M, et al. **Increasing the visibility of thin NITINOL vascular implants.** *Current Directions in Biomedical Engineering* 2015;1:503–06 [CrossRef](#)